

Structure of ^{33}S from a study of the $^{34}\text{S}(p, d)^{33}\text{S}$ reaction at 35 MeV*

A. Moalem and B. H. Wildenthal

Cyclotron Laboratory, Michigan State University, East Lansing, Michigan 48824

(Received 25 September 1974)

The $^{34}\text{S}(p, d)^{33}\text{S}$ reaction has been studied at a proton energy of 35 MeV. Deuteron spectra were analyzed in a magnetic spectrograph with an over-all energy resolution, full width at half-maximum, of about 8 keV. Excitation energies were measured for levels in ^{33}S through 7.5 MeV excitation with an accuracy of $\pm(1.0 \text{ keV} + 0.5 \text{ keV per 1 MeV of excitation})$. Values of the orbital angular momenta of neutrons transferred in these transitions, and the corresponding spectroscopic factors, were extracted from the data by means of distorted-wave Born-approximation calculations. Several new $J^\pi = \frac{1}{2}^+$ assignments were made. The experimental results are compared to the predictions of current nuclear structure theories for this nucleus.

NUCLEAR REACTIONS $^{34}\text{S}(p, d)$, $E_p = 35 \text{ MeV}$; measured $\sigma(E_d, \theta)$; enriched target; deduced energies, l_n values, and spectroscopic factors for states of ^{33}S .

I. INTRODUCTION

The properties of the low-excitation-energy states of ^{33}S have been studied rather extensively with particle-transfer reactions,¹⁻⁷ which have mapped out most of their dominant one- and two-particle features, and with various γ -ray-decay experiments,⁸⁻¹² which have yielded a detailed picture of their electromagnetic features. The observed properties of this nucleus have been interpreted in terms of strong-coupling rotational models,¹³ weak-coupling vibrational models,¹⁴ and several mixed-configuration shell models.¹⁵⁻¹⁷ The qualitative structure features of ^{33}S and its neighbors do not offer unambiguous guidance as to what theoretical approach would be most satisfactory for this region. Hence choices as to the most advantageous theoretical approach to interpreting the data must be made in large part on the basis of detailed comparisons between observed and predicted phenomena.

The most extensive comparisons between theory and experiment for ^{33}S have been made for the shell-model wave functions of Ref. 17. Those results were obtained by diagonalizing two different Hamiltonians, one constrained to the modified surface δ interaction form (MSDI) and one a combination of free and surface δ elements (FPSDI), in a space spanned by those configurations $d_{5/2}^{n_1} s_{1/2}^{n_2} d_{3/2}^{n_3}$ for which $n_1 \geq 10$. At the present level of knowledge, it appears that this approach, of using a large, albeit moderately truncated, basis space which includes configurations of all three sd -shell orbits, together with a Hamiltonian that gives consistent agreement between calculated and observed level energies for several neighboring nuclei, gives the best representation of ob-

served phenomena.

The present study has two aims. One is to make a reasonably definitive catalog of the levels of ^{33}S which can be excited in a pickup reaction and, where possible, to extend the list of spin-parity assignments of these levels. The other is to derive a set of spectroscopic factors for single-nucleon pickup to ^{33}S from ^{34}S to supplement those previously available.¹ New or more reliable information in either of these areas will provide still more rigorous constraints on what can be considered as an adequate theoretical accounting for this system.

II. EXPERIMENTAL PROCEDURES

The present experiment was carried out with 35 MeV protons from the Michigan State University sector-focused cyclotron. The uncertainty in the absolute calibration of the beam energy was $\sim 50 \text{ keV}$. The deuterons were analyzed with an Enge split-pole magnetic spectrograph and spectra were recorded alternatively with nuclear emulsions (two abutting 25 cm long plates) and a 20 cm long single-wire position-sensitive gas proportional counter. The nuclear emulsions were used to obtain spectra with high energy resolution and precise excitation-energy calibration. The proportional-counter spectra were limited to a resolution of 50 keV, full width at half-maximum (FWHM), by the characteristics of the counter, but these spectra were very useful supplements to those recorded on the emulsions, especially for intense peaks which sometimes could not be counted accurately because of too high a density of track images.

The beam currents on target for this experi-

ment ranged between 300 and 800 nA and had a (coherent) energy spread of about 20 keV. With the utilization of dispersion matching and the other techniques described by Blosser *et al.*,¹⁸ a resolution of 8 keV, FWHM, for 25 MeV deuterons was obtained at the spectrograph focal plane, as recorded on the nuclear emulsion plates. The target used in this experiment was a thin ($\approx 10 \mu\text{g}/\text{cm}^2$) layer of enriched ^{34}A (85.5% ^{34}S , 0.5% ^{33}S , and 14% ^{32}S) sandwiched between layers of carbon and Formvar foils.

III. EXPERIMENTAL RESULTS

A. Excitation energies

A typical spectrum of the present (p, d) data, as recorded with nuclear emulsions, is shown

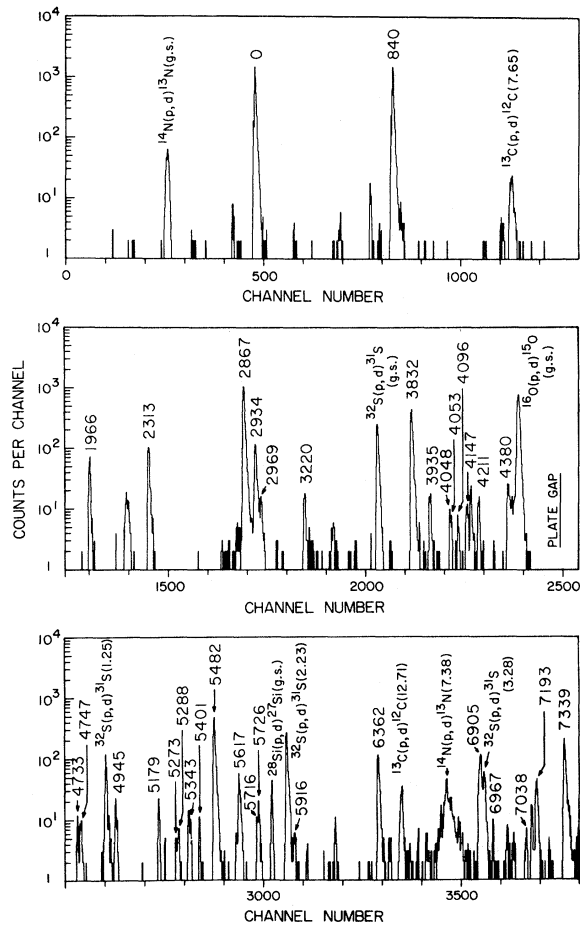


FIG. 1. Spectrum of deuterons from the $^{34}\text{S}(p, d)^{33}\text{S}$ reaction, measured at $E_p = 35 \text{ MeV}$ and $\theta_{\text{lab}} = 20^\circ$ with nuclear emulsions. The resolution (FWHM) of the peaks from sulfur is $\approx 8 \text{ keV}$. Excitation energies in keV, as obtained in the present work, label the peaks corresponding to states of ^{33}S . Other labels denote peaks from some of the more prominent target contaminants.

in Fig. 1. The excitation energies obtained in the present work are used to label the peaks corresponding to excited states of ^{33}S . The identification of a peak with a state in ^{33}S was made only after a careful check on its appearance and measured excitation energy at several different angles of observation. This care was necessary because the thinness of the target combined with the relatively large amount of material in the "bread" of the sandwich made the strength of contaminant groups relative to those of primary interest larger than usual. The nuclear emulsions were shielded from $Z \geq 2$ particles, but protons, deuterons, and tritons were all recorded and used to help establish the final energy calibration of the spectrograph focal plane.

The excitation energies we assign to levels in ^{33}S are based on a final calibration of the spectrograph focal plane obtained by adjusting the various parameters which affect the calculated values of emergent-particle momenta in our reaction-particle kinematics program about their nominal values so as to obtain a least-squares fit of the excitation energies (total Q values) of selected reference states to accurately known values. Parameters which are varied in this procedure are the beam energy, angle of observation, gap between abutting plates, and the linear and quadratic parameters of the B_p vs focal plane-position relationship for the spectrograph.¹⁹ In the fitting procedure we used deuteron groups from the ground state transitions of the ^{34}S , ^{28}Si , ^{16}O , ^{14}N , and $^{12}\text{C}(p, d)$ reactions, and proton groups from elastic scattering on ^{12}C and ^{16}O and from inelastic scattering to the first excited states in ^{32}S and ^{34}S . These groups span more than the entire region of excitation energies studied in ^{33}S . The inclusion of both deuteron and proton groups and of reactions on a significant range of target masses makes an accurate determination of the beam energy and scattering angle possible. The inclusion of (p, d) groups leading to several low-lying excited states of ^{33}S , whose excitation energies are known to $\pm 1 \text{ keV}$ accuracy from Ge(Li) detector studies of their γ -ray decays, leaves the results of the adjustment essentially unchanged.

The uncertainties which reside in this procedure were estimated from trials with several different target nuclei, from trials for a particular target with several different combinations of input "known energy" particle groups, and from trials with the same "reference data set" at several different angles of observation, again for a particular target. The standard deviations in the assigned Q values obtained from analyzing a specific set of scanning results with a specific set of reference peaks are of the order of 0.8 keV. The uncertain-

TABLE I. Excitation energies, J^π and l values, and pickup spectroscopic factors for states of ^{33}S .

	E_x (keV)	J^π	l	$100 \times C^2 S(l, j)$		
				Experiment	FPSDI (Ref. 17)	MSDI (Ref. 17)
0 ^a	0 ^b	$\frac{3}{2}^+$ a, b	2 ^a	187 ^c	187	176
840	840.4 ± 0.3	$\frac{1}{2}^+$	0	80	85	98
1966	1966.4 ± 0.3	$\frac{5}{2}^+$	2	5	17	5
2313	2312.6 ± 0.4	$\frac{3}{2}^+$	2	17	25	15
2867	2866.3 ± 0.3	$\frac{5}{2}^+$	2	127	158 ($\frac{5}{2}^+$)	90
2934	2934.3 ± 0.5	$\frac{7}{2}^-$	3	2		
2969	2968.7 ± 0.4	$\frac{7}{2}^+$	(4)			
3220	3219.5 ± 0.9	$\frac{3}{2}^-$	1	2		
3832	3830 ± 2	$(\frac{5}{2}, \frac{3}{2})^+$	2	59	0 ($\frac{5}{2}^+$)	40
3935	3934 ± 3	$(\frac{5}{2}, \frac{3}{2})^+$	2	2	6 ($\frac{3}{2}^+$)	8
4048	4047.6 ± 1.0	$\frac{9}{2}^+$	(4)			
4053	4053 ± 3	$\frac{1}{2}^+$	0	0.3	10	6
4096	4093.8 ± 1.0	$\frac{7}{2}^+$				
4147	4143 ± 3	$(\frac{3}{2}^+, \frac{5}{2})$			13 ($\frac{5}{2}^+$)	22
4211	4212 ± 2	$\frac{3}{2}^-$				
4380	4377 ± 5	$\frac{1}{2}^+$	0	3	15	0
4425	4426 ± 5					
4733	4732 ± 6	$(\frac{5}{2}, \frac{9}{2})$				
4747	4747 ± 6					
	4869 ± 6	$\frac{11}{2}^-$				
	4920 ± 2	$\frac{1}{2}^-$				
4945	4941 ± 6	$(\frac{5}{2}, \frac{7}{2})^-$	3	5		
5179	5177 ± 6		(3, 4)			
	5210 ± 6					
5273	5272 ± 6					
5288	5287 ± 6					
5343	5340 ± 6	$(\frac{5}{2}, \frac{3}{2})^+$	2	3		
	5351 ± 6					
5401	5399 ± 6					
5482	5475.4 ± 1.4	$\frac{1}{2}^+, T = \frac{3}{2}$	0	46	40	35
	5599 ± 5					
	5613 ± 6					
5617	5622 ± 6	$\frac{1}{2}^+$	0	10		
5716	5155 ± 2	$\frac{1}{2}^-$				
5726			(4)			
	5864 ± 6					
	5893 ± 2	$\frac{3}{2}^-$				
5916 ^d	5915 ± 6	$\frac{1}{2}^+$	0	1		

TABLE I (Continued)

E_x (keV)	J^π	l	$100 \times C^2S(l, j)$		
			Experiment	FPSDI (Ref. 17)	MSDI (Ref. 17)
5982 ± 6					
6362	6360 ± 6	$(\frac{3}{2}, \frac{5}{2})^+$	2	21	
6905	6892 ± 6	$(\frac{3}{2}, \frac{5}{2})^+, T = \frac{3}{2}$	2	35	18 ($\frac{3}{2}^+$)
6967	6965 ± 6				
7038	7037 ± 6				
7193	7193 ± 2	$\frac{3}{2}^-$			
7339	7344 ± 12	$(\frac{3}{2}, \frac{5}{2})^+, T = \frac{3}{2}$	2	41	40 ($\frac{5}{2}^+$)

^a Present work; uncertainties are $\pm(1.0 + 0.5E_x \text{ MeV/keV})$.

^b References 7, 11, 12; energies are those of Ref. 7.

^c Relative values from present work; see Table III for absolute values.

^d Many experimental levels not listed here are tabulated in Ref. 7 above 6.0 MeV excitation.

ties in the reproducibility of the assigned relative positions of peaks on the emulsion plates amount to approximately 0.6 keV (0.02 mm), leading to an inherent uncertainty in our data of about 1 keV. The remainder of the uncertainty in our Q -value assignments arises from the amount of reference-data information available, and the various accuracies thereof. The typical uncertainties in the energies used for the reference peaks were of the order of 1 to 2 keV. In the region of excitation in ^{33}S from 4 to 7 MeV, the relative paucity of reference data enlarges this uncertainty somewhat. Our estimate for the errors in the energies we assign is thus $\pm 1.0 + 0.5 \text{ keV/MeV}$ of excitation. The values of the excitation energies of ^{33}S obtained in this work are presented in Table I, together with the consensus values arrived at in Ref. 7.

B. Angular distributions

For relatively strong and/or well-isolated states in ^{33}S , the differential cross sections measured with nuclear emulsions and with the proportional counter were combined to form the final experimental angular distributions. In the cases for which the limited resolution of the wire counter vitiated data from that source, the angular distributions presented come solely from the emulsion data.

The angular distributions obtained for states of ^{33}S are shown in Figs. 2–6. The cross-section normalization for these differential cross sections was established from measurements of the elastic scattering from the target in the $\theta_{\text{lab}} = 30^\circ\text{--}55^\circ$ range under identical experimental conditions to those used in the wire-counter measurements of the (p, d) transitions. The elastic scattering rates were assumed to be equal to the correspond-

ing differential cross sections calculated in the optical model with the parameters of Becchetti and Greenlees,²⁰ thus fixing the relation between experimental counting rates and cross sections.

The measured shape of the elastic scattering angular distribution in the $\theta_{\text{lab}} = 30^\circ\text{--}50^\circ$ region agrees with the Becchetti-Greenlees predictions both for this and other sd -shell nuclei. We estimate the uncertainty in the normalization at these angles of the optical model predictions as 10%, and allow an independent 10% uncertainty for errors in the data and the mechanics of normalizing the experimental numbers to the theory. Thus, we think the assigned experimental cross section scale is good to at least 15%. The uncertainties in the relative normalizations from one state to another range from 2 to 5%.

IV. DWBA ANALYSIS

The angular distributions measured for $^{34}\text{S}(p, d)^{33}\text{S}$ in the present experiment were analyzed by comparing them to predictions of distorted-wave Born-approximation (DWBA) calculations made with the code DWUCK.²¹ From these comparisons, assignments of the orbital angular momenta, l_n , transferred in the pickups can be assigned, and thus the parity and possible J values of the residual levels inferred. The ratios of the measured cross sections to those calculated in the DWBA provide the reduced strengths, or spectroscopic factors, for the various transitions, according to the formula

$$\frac{\sigma(\theta)_{\text{exp}}(2j+1)}{\sigma_{ij}(\theta)_{\text{DWUCK}}} = 2.29C^2S_{ij}.$$

In all of the DWBA calculations, the bound-state wave functions of the transferred neutrons were generated as eigenfunctions of a Woods-

Saxon potential with the conventional spin-orbit term. The depths of the potential were adjusted to reproduce the experimental separation energies of the various transitions. All calculations employed the finite-range and nonlocality (FRNL) approximate corrections as suggested in Ref. 21.

The optical model parameters used for the proton channel in the DWBA calculations were those of Ref. 20. The choice of the most appropriate

optical model parameters for the deuteron channel is much more difficult than for the proton case. Not only are there fewer data and less extensive global analyses of these data, but there is also some question theoretically²² as to whether it is even correct to use deuteron parameters which reproduce deuteron elastic scattering in a DWBA calculation of (p, d) or (d, p) reactions.

A survey²³ of the results obtained in DWBA calculations for (p, d) reactions on sd -shell nuclei has led to the conclusion that deuteron elastic scattering optical model potentials close to those

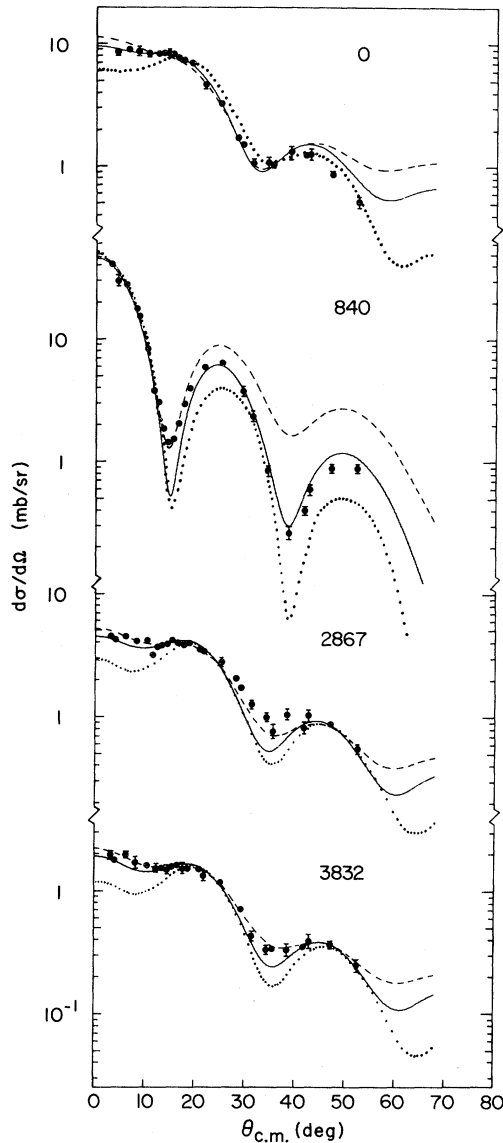


FIG. 2. Results of different DWBA formulations. The solid and dashed curves indicate results of approximate FRNL calculations, made with an orthodox deuteron potential ($D1$), with and without the effect of the density-dependent p - n interaction, respectively. The dotted curves indicate results obtained with the adiabatic deuteron potential ($D3$).

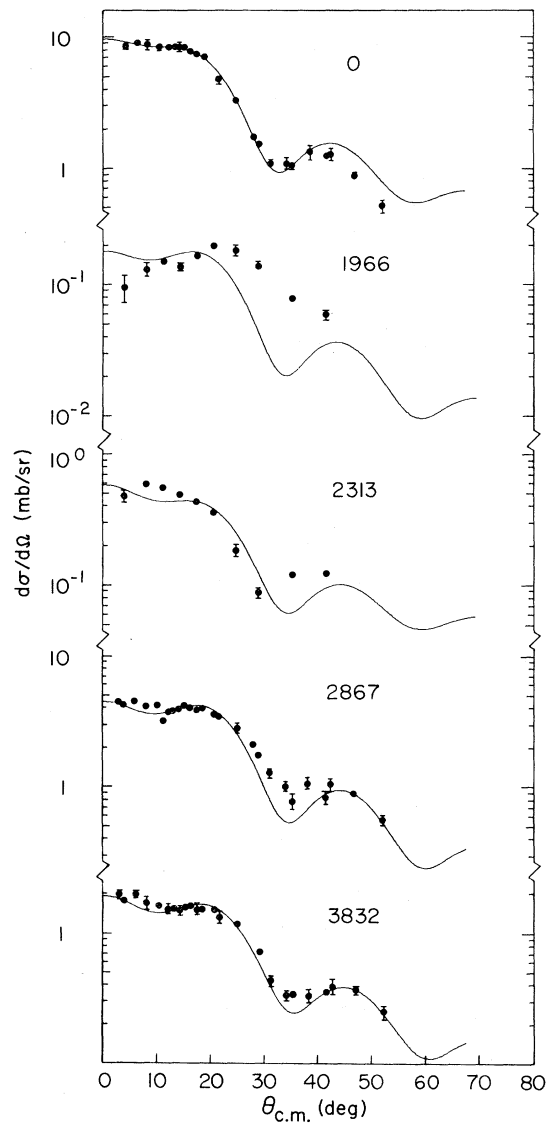


FIG. 3. Angular distributions for low-lying $l=2$ transitions. The curves indicate approximate FRNL DWBA calculations with deuteron potential $D1$ and density dependence.

of Newman *et al.*,²⁴ and Hinterberger *et al.*,²⁵ do best among the various choices available in the literature in reproducing the observed angular distributions of small ($l=0, 1$, and 2) l_n transfer.

All of the conventional deuteron potentials produce calculated distributions corresponding to our data which fail to fall off fast enough at angles $\geq \theta_{\text{c.m.}}=30^\circ$. The use of a deuteron potential adjusted so as to account for disassociation of the deuteron into relative S waves (the Johnson-Soper or "adiabatic" potential)²² tends to produce cal-

culated angular distributions which decrease rapidly at angles larger than 30° and has had striking success in improving the agreement between DWBA predictions and experimental data for closed-shell nuclei.^{26, 27} Another avenue towards obtaining better agreement between DWBA predictions for (p, d) and the data beyond 30° is to introduce the effects of a damping of the p - n

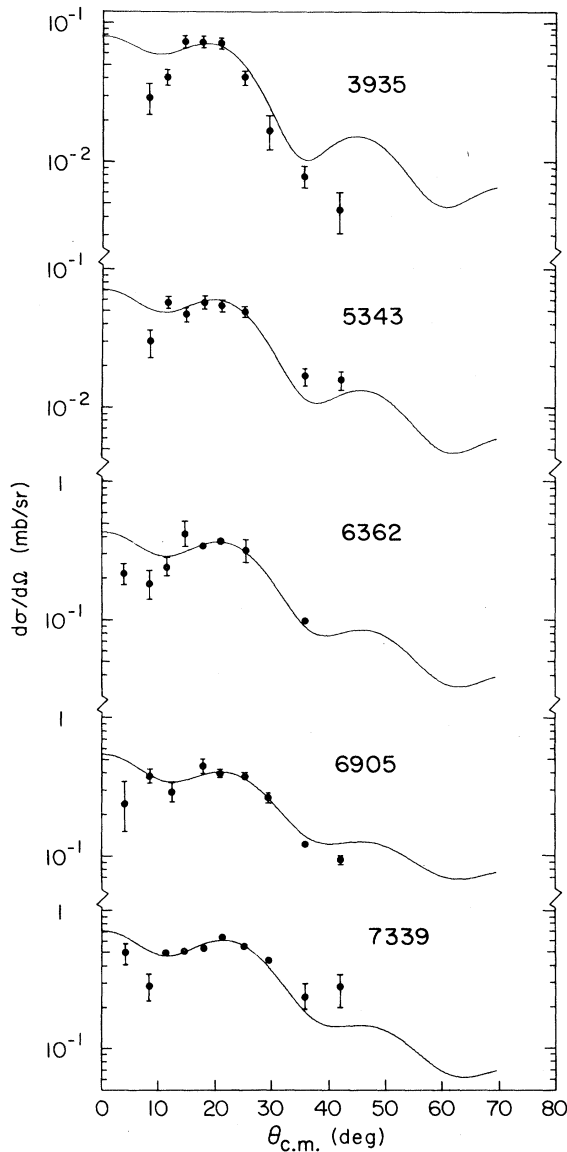


FIG. 4. Angular distributions for higher-lying $l=2$ transitions. The curves indicate approximate FRNL DWBA calculations with deuteron potential $D1$ and density dependence.

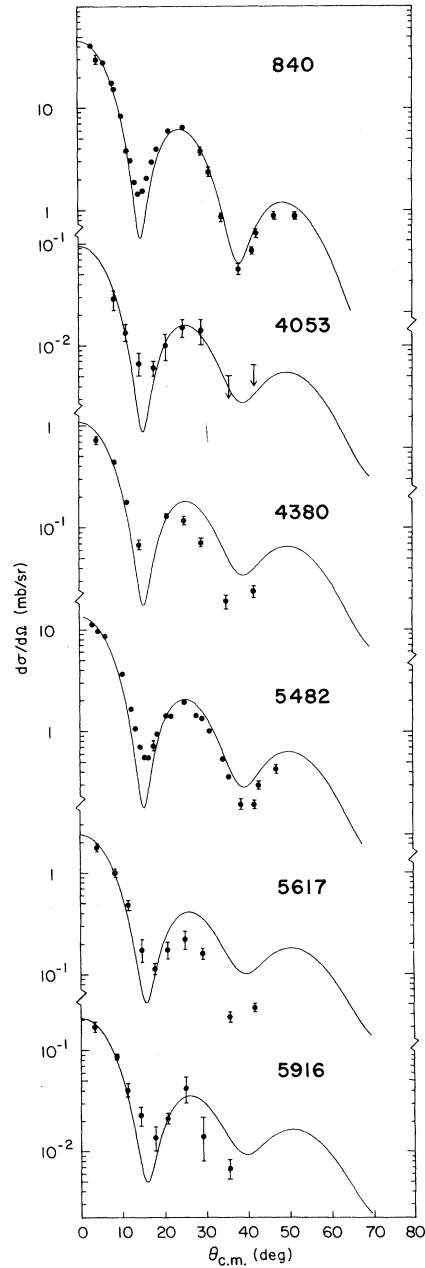


FIG. 5. Angular distributions of $l=0$ transitions. The solid lines indicate approximate FRNL DWBA calculations with deuteron potential $D1$ and density dependence.

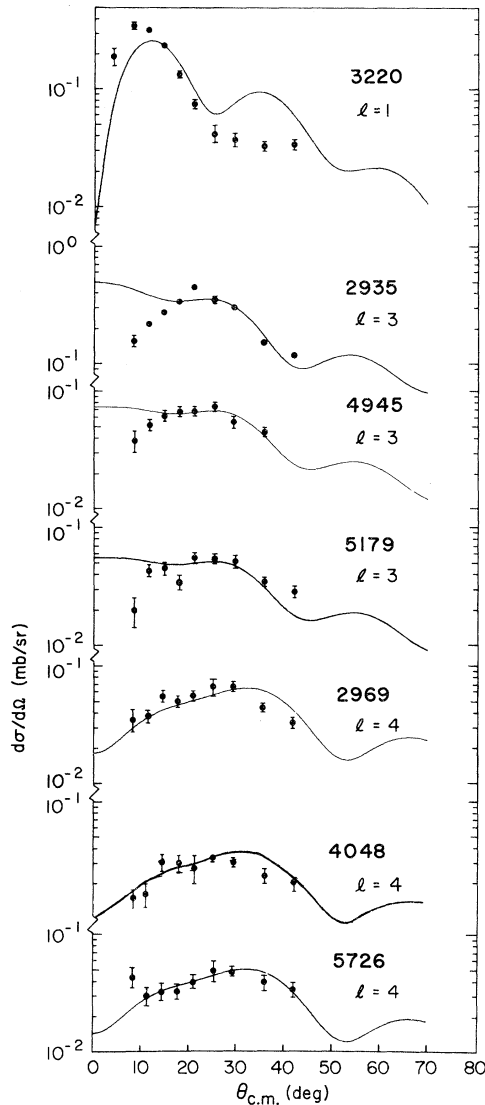


FIG. 6. Angular distributions of other than $l=0$ and 2 transitions. The solid curves indicate approximate FRNL DWBA calculations with deuteron potential $D1$ and density dependence.

interaction as a function of the density of the nucleus.²⁸ This "density-dependence" effect enters the calculation by means of a smooth reduction of the form factor as a function of radius.²⁹

In Fig. 2 we show results from three sets of calculations. One family of calculations is completely standard and employs the Becchetti-Greenlees²⁰ proton parameters and the Hinterberger *et al.*,²⁵ deuteron parameters ($D1$). The second family of calculations employs the same set of optical potentials but introduces the density-dependence effects. The third family is different from the first in that a Johnson-Soper²² deuteron potential ($D3$) is substituted for the Hinterberger potential. The values of the various optical model parameters are listed in Table II.

We have chosen the "density-dependence" calculations to compare to the full set of experimental angular distributions in Figs. 3-6 and to use in obtaining the spectroscopic factors listed in Table I. The differences in relative and absolute spectroscopic factors which result from using the alternate DWBA formulations are shown in Table III.

V. DISCUSSION OF RESULTS

A. Level energies and spin-parity assignments

We identify in this work at most one level (at 5726 keV) in ^{33}S which was previously unknown. Nine of the 37 previously identified⁷ levels below 6.0 MeV excitation were not populated strongly enough to be clearly identified from our data. Our energy assignments are in good agreement with the consensus values⁷ up through 4 MeV of excitation. Above that energy our values are in good agreement with the ± 6 keV values of Endt,⁵ obtained with the (d, p) reaction, but disagree by 2 standard deviations with the energy of 5.475 ± 0.0014 MeV quoted⁷ for the lowest $T = \frac{3}{2}$ level.

We were able to make very significant new assignments of $\frac{1}{2}^+$ to levels at 4.053, 4.380, and

TABLE II. Optical-model parameters used in the DWBA analysis of $^{34}\text{S}(p, d)^{33}\text{S}$ at $E_p = 35$ MeV.

	V_r (MeV)	r (fm)	a (fm)	W_v (MeV)	W_{sf} (MeV)	f' (fm)	a' (fm)	V_{s0} (MeV)	r_s (fm)	a_s (fm)	r_c (fm)
Protons ^a	44.10	1.17	0.75	5.0	3.39	1.32	0.53	6.2	1.17	0.75	1.25
$D1$ ^b	78	1.25	0.73	...	13.00	1.25	0.75	6	1.25	0.75	1.30
$D2$ ^c	95.44	1.08	0.80	...	11.81	1.34	0.76	6.31	1.02	0.80	1.30
$D3$ ^d	103.16	1.17	0.79	1.19	17.33	1.29	0.56	6.2	1.17	0.75	1.30
Bound state		1.25	0.65					5.0			

^a Reference 20.

^b Reference 24.

^c Reference 25.

^d References 22, 26, 27, and 20.

5.916 MeV. These assignments were made possible by the conjunction of our high-resolution spectra at very forward angles and the unique order-of-magnitude rise in the differential cross section of the $l=0$ shape as the angle of observation is moved from $\theta_{\text{lab}}=15^\circ$ to 4° . The unambiguous nature of the assignments can be seen from Fig. 5.

Our data also confirm the previously tentative $l=2$ character of the second and third $T=\frac{3}{2}$ states at 6.905 and 7.339 MeV (see Fig. 4). Beyond $l=0$ and $l=2$ assignments, few conclusive results can be obtained from the DWBA fits. The level at 3220 keV, known to be $\frac{3}{2}^-$ and to have a dominant $2p_{3/2}$ single-particle character, has a clear $l=1$ shape. Likewise, the $f_{7/2}$ single-particle state at 2935 keV has been an $l=3$ shape. The DWBA predictions fit these observed shapes with only moderate success. In particular, the calculated $l=3$ shape does not fall off as it should at forward angles. (This feature of $l=3$ distributions is one that persists over several nuclei and a wide variety of calculations.) The $\frac{7}{2}^+$ and $\frac{9}{2}^+$ assignments to the states at 2969 and 4048 keV, respectively, are consistent with the rather inconclusive fits of $l=4$ shapes to the distributions observed for these transitions. The $l=1, 3,$ and 4 results can be seen in Fig. 6.

The theoretical energy level spectra of ^{33}S presented in Ref. 17 can be evaluated in considerably more detail with the aid of the present new assignments and other new results compiled in Ref. 7. From the FPSDI spectrum, the first predicted $\frac{7}{2}^+$ (2.71 MeV) and $\frac{9}{2}^+$ (3.81 MeV) states are now seen to closely match the experimental states observed at 2.969 and 4.048 MeV. The second predicted $\frac{7}{2}^+$ (3.65 MeV) is not too far off from the second observed $\frac{7}{2}^+$ state at 4.094 MeV. The spectrum contained three $\frac{1}{2}^+$ states in the 4–5 MeV region, (3.78, 4.47, and 4.63 MeV), none of which had been observed at the time. Since it might be expected that $\frac{1}{2}^+$ states would have been observed

in the previous transfer reactions, the discrepancy as it existed in Ref. 17 was one of the worst breakdowns of that shell-model calculation, because the nonobservance of a predicted level is a more serious failure of the theoretical model than is the converse situation. The fact that at least two of these predicted $\frac{1}{2}^+$ states are now observed at energies quite close to the predicted values is a very nice validation of the shell-model calculations. The fourth $\frac{1}{2}^+$ state observed at 5.617 is far enough away from the fourth predicted level to leave their correspondence doubtful.

B. Spectroscopic factors

The spectroscopic factors obtained in the present work are presented (in relative values) in Table I, along with the theoretical predictions of Ref. 17. The consistency with which the spectroscopic factors are extracted from the data via DWBA analysis can be inferred from Table III. Also noted in Table III are the normalizing factors by which the absolute values of the spectroscopic factors obtained from the present experiment and the DWBA values from various calculations must be multiplied to obtain a value of $S=1.87$ for the ground state. For the purpose of all further comparison and discussion, the spectroscopic factors are presented in this renormalized form, so that the ground state value is equal to the FPSDI value of Ref. 17.

The FPSDI wave function¹⁷ for $^{34}\text{S}(\text{g.s.})$ has occupation probabilities $\langle d_{5/2} \rangle = 11.4$, $\langle s_{1/2} \rangle = 3.4$, and $\langle d_{3/2} \rangle = 3.2$; the $^{33}\text{S}(\text{g.s.})$ spectroscopic factor of 1.87 thus exhausts more than half of the total strength for $d_{3/2}$. This state is, to a good approximation, a $d_{3/2}$ hole coupled to $^{34}\text{S}(\text{g.s.})$, as it is also a $d_{3/2}$ particle coupled to $^{32}\text{S}(\text{g.s.})$. Relative to the $\frac{3}{2}^+$ ground state, the model wave functions predict spectroscopic factors for the next higher two $\frac{3}{2}^+$ states that are somewhat too large, although

TABLE III. Comparison of spectroscopic factors obtained from different DWBA analysis. The parameters Sets $D1, D2,$ and $D3$ are defined in Table II. The results from the "density-dependent" calculations are denoted by the DD.

E_x (keV)	FRNL			FRNL-DD		$(^3\text{He}, ^4\text{He})^a$
	$D1$	$D2$	$D3$	$D1$	$D2$	
0	187	187	187	187	187	190
840	99	70	71	80	66	65
2867	132	127	149	127	121	90
3832	63	60	67	59	67	50
5485	61	48	42	46	40	47
Normalization factor	0.67	0.52	0.71	0.46	0.42	

^a Reference 1.

the qualitative agreement with the experimental results is not bad. The amount of $d_{3/2}$ strength predicted for the lowest FPSDI $T = \frac{3}{2}^+ J^\pi = \frac{3}{2}^+$ state is significantly lower than the observed strength. This quantity appears to be rather sensitive to the details of the nuclear Hamiltonian, as can be seen from the much larger MSDI value. Over all, the present experimental results for $d_{3/2}$ favor the MSDI over the FPSDI wave functions.

Relative to the $\frac{3}{2}^+$ ground state, the strength observed for the lowest $T = \frac{1}{2}$ and $T = \frac{3}{2}$ $J^\pi = \frac{1}{2}^+$ states are in excellent agreement with the FPSDI results. The MSDI predictions are not badly off, but agreement with experiment is not as striking as for the FPSDI results. These lowest $\frac{1}{2}^+$ states can be thought of, then, as the $T = \frac{1}{2}$ and $T = \frac{3}{2}$ couplings of an $s_{1/2}$ hole to the $T = 1$ $^{34}\text{S}(\text{g.s.})$ wave function. The FPSDI predictions for the higher $\frac{1}{2}^+$ states are too large, as was the case for the $\frac{3}{2}^+$ states, while the MSDI prediction do a little better in this regard.

The ratio of total $s_{1/2}$ strength observed relative to $d_{3/2}$ strength is in good agreement with the shell-model apportionment for the region sampled by the experiment. It might be noted that the two-to-one enhancement of $d_{3/2}$ pickup relative to $s_{1/2}$ pickup for the $T = \frac{1}{2}$ states, as compared to the less than one-to-one ratio for $T = \frac{3}{2}$, can be understood qualitatively from the plausible assumption that the extra two neutrons of ^{34}S tend to occupy the "last" shell-model orbit $d_{3/2}$. Hence for the $T = \frac{1}{2}$ states, which can only be reached from ^{34}S by neutron pickup, we can expect that the $d_{3/2}$ strength is enhanced over what occurs for the $T = \frac{3}{2}$ states, which are reached equivalently by proton and neutron pickup. Nature and the shell-model results thus indicate that while the simplistic picture of $^{34}\text{S}(\text{g.s.})$ as $(d_{5/2})^{12}(s_{1/2})^4 d_{3/2}^2$ is in reality significantly altered, e.g., we do observe significant $d_{3/2}$ pickup to the $T = \frac{3}{2}$ $J^\pi = \frac{3}{2}^+$ state, the basic flavor of the zero-order model is still there. The fact that the $T = \frac{3}{2}$ strength for $d_{3/2}$ pickup must arise completely from configuration mixing makes the relative theoretical instability of this quantity more understandable.

The experimental and theoretical values for $d_{5/2}$ spectroscopic factors are probably the most interesting of this set of results, since they yield qualitatively a definitive index of the shell-model basis-space requirements and also yield a strong constraint upon the model Hamiltonian having the proper general characteristics. Unless the $d_{5/2}$ orbit is included in the active model basis space, no $\frac{5}{2}^+$ state can have pickup strength. If none of the low-lying $\frac{5}{2}^+$ states exhibited significant pickup strength, this would be evidence that the $d_{5/2}$ orbit could be omitted from explicit considerations and

its influence treated by a renormalization of the Hamiltonian. The first observed $\frac{5}{2}^+$ state (1966 keV) does have a very small pickup spectroscopic factor, which indicates that its wave function can quite plausibly be constructed by recoupling $d_{3/2}$ and $s_{1/2}$ particles.

The second possible $\frac{5}{2}^+$ state (2866 keV), however, has a pickup strength equal to that of the ground and first excited $\frac{3}{2}^+$ and $\frac{1}{2}^+$ states. While the spin assignment of this state is not conclusively $\frac{5}{2}^+$ from rigorous experimental arguments, we assume it to be so henceforth. Not only would a $\frac{3}{2}^+$ assignment be incomprehensible from shell-model arguments based both on specific calculations and on sum rules, but there is even experimental evidence (though not rigorous) for a $\frac{5}{2}^+$ assignment from the present data, which show the rather slight but clear broadening of the slope down from the $l=2$ maximum which is characteristic of $d_{5/2}$, as opposed to $d_{3/2}$ $l=2$ transfer. This $\frac{5}{2}^+$ state is not as pure a "hole" state as are the $\frac{3}{2}^+$ and $\frac{1}{2}^+$ ground and first excited states (it contains only approximately 10% of the total $d_{5/2}$ -hole strength as opposed to the 25–50% for the other two states) but $[^{34}\text{S}(\text{g.s.})] \times [d_{5/2}^{-1}]$ is certainly the dominant characteristic of its wave function. The same arguments which we applied to the 2866 keV state can be applied, though without as much force, to the 3830 keV state. The spectroscopic factor of 0.6 definitely implies that the $d_{5/2}$ -hole characteristic is one of this state's important features.

It is an important success that the shell-model calculations of Ref. 17 correctly place $d_{5/2}$ -hole strength of about 1.5 units in the vicinity of the second $\frac{5}{2}^+$ state. This result is the primary evidence for the effective $d_{5/2}$ -($d_{3/2}$ and $s_{1/2}$) orbit-orbit interaction in this region, and it is quite easy for a Hamiltonian which does not correctly account for this interaction to predict no $d_{5/2}$ -hole strength at all at this excitation. In detail, the FPSDI and MSDI results must share this success, with the MSDI results more accurately reproducing the fragmentation of the strength and the FPSDI results better reproducing the total strength observed.

In the $T = \frac{3}{2}$ system, the *first* $\frac{5}{2}^+$ state is seen to have the $d_{5/2}$ -hole feature as its dominant characteristic. (Again we assume $\frac{5}{2}^+$ for the 7339 keV state in the absence of a rigorous choice of $\frac{5}{2}^+$ over $\frac{3}{2}^+$.) For this state there is perfect agreement between the two different shell-model results and the present experimental value. Finally, to conclude our discussion of the $\frac{5}{2}^+$ states, we note that the total $d_{5/2}$ pickup strength observed is only about 30% of the total possible strength, as opposed to ~100% for the cases of $d_{3/2}$ and $s_{1/2}$. The fact that the shell-model results predict this feature

quite accurately, a feature which, for example, is quite beyond the scope of any general sum-rule arguments, is a significant virtue of a detailed microscopic nuclear model.

VI. CONCLUSIONS

The angular distributions of the (p, d) reaction observed at $E_p = 35$ MeV on a ${}^{34}\text{S}$ target can be fitted quite well with conventional DWBA calculations if the appropriate deuteron optical-model potentials (those which best fit elastic scattering data) are used. Data in the far-forward (4° – 20°) region, not usually measured, do not favor the adiabatic-deuteron model of Johnson and Soper, even though this approach works very well for the larger-angle data. Introduction of a density-dependent damping factor in the p - n interaction

(which effectively dampens the form factor in the interior) produces the best fits to the observed distributions. The spectroscopic factors extracted with the DWBA have a relative scatter of 5–15% over a range of l and Q value as a function of optical-model choice. The agreement of the present results with those from the $({}^3\text{He}, \alpha)$ reaction is within ~25%.

Both the general and specific features of the pickup spectroscopic factor results are well accounted for by recent shell-model calculations. Except for minor points, it would appear that agreement between shell model and experiment for this system is good enough that further improvement in the structure calculations could not be conclusively verified because of the residual ambiguities in the DWBA-extracted experimental spectroscopic factors.

*Work supported in part by the U. S. National Science Foundation.

¹H. G. Leighton and A. C. Wolff, Nucl. Phys. A151, 71 (1970).

²J. Dubois, Nucl. Phys. A117, 533 (1968).

³A. Graue *et al.*, Nucl. Phys. A162, 593 (1971).

⁴K. T. Knopfle *et al.*, Phys. Rev. C 4, 818 (1971).

⁵P. M. Endt and C. H. Paris, Phys. Rev. 110, 89 (1958).

⁶M. C. Mermaz *et al.*, Phys. Rev. C 4, 1778 (1971).

⁷P. M. Endt and C. van der Leun, Nucl. Phys. A214, 1 (1973).

⁸R. G. Hirko and A. D. W. Jones, Nucl. Phys. A192, 329 (1972).

⁹J. E. Cummings and D. J. Donahue, Phys. Rev. C 2, 942 (1970).

¹⁰J. A. Becker, L. F. Chase, Jr., D. B. Fossan, and R. E. McDonald, Phys. Rev. 146, 761 (1966).

¹¹P. E. Carr *et al.*, J. Phys. A, 6, 685 (1973).

¹²P. A. Butler *et al.*, J. Phys. A, 6, L15 (1973).

¹³P. Taras, Can. J. Phys. 44, 1563 (1966).

¹⁴B. Castel, K. W. C. Stewart, and M. Harvey, Nucl. Phys. A162, 273 (1971).

¹⁵P. W. M. Glaudemans, G. Wiechers, and P. J. Brussaard, Nucl. Phys. 56, 529, 548 (1964).

¹⁶M. C. Bouten, J. P. Elliot, and J. A. Pullen, Nucl. Phys. A97, 113 (1967).

¹⁷B. H. Wildenthal, J. B. McGrory, E. C. Halbert, and H. D. Graber, Phys. Rev. C 4, 1708 (1971).

¹⁸H. G. Blosser, G. M. Crawley, R. deForest, E. Kashy, and B. H. Wildenthal, Nucl. Instrum. Methods 91, 61 (1971).

¹⁹J. A. Nolen, Jr., G. Hamilton, E. Kashy, and I. D. Proctor, Nucl. Instrum. Methods 115, 189 (1974).

²⁰F. D. Becchetti and G. W. Greenlees, Phys. Rev. 182, 1190 (1969).

²¹P. D. Kunz, University of Colorado Report, 1967 (unpublished).

²²R. C. Johnson and P. J. R. Soper, Phys. Rev. C 1, 976 (1970); J. D. Harvey and R. C. Johnson, *ibid.* 3, 636 (1971).

²³J. A. Rice, Ph.D. thesis, Michigan State University, 1973 (unpublished).

²⁴E. Newman, L. C. Becker, B. M. Preedom, and J. C. Hiebert, Nucl. Phys. A100, 225 (1967).

²⁵F. Hinterberger *et al.*, Nucl. Phys. A111, 265 (1968).

²⁶G. M. McAllen, W. T. Pinkston, and G. R. Satchler, Particles and Nuclei 1, 412 (1971).

²⁷G. R. Satchler, Phys. Rev. C 4, 1485 (1971).

²⁸A. M. Green, Phys. Lett. 24B, 384 (1967).

²⁹B. M. Preedom, J. L. Snelgrove, and E. Kashy, Phys. Rev. C 1, 1132 (1970); B. M. Preedom, *ibid.* 5, 587 (1972).